# Reduced Pd density of states in Pd/SAM/Au junctions: the role of adsorbed hydrogen atoms

Jan Kučera and Axel Groß
*Institute for Theoretical Chemistry, Ulm University, D-89069 Ulm/Germany*

Experiments have shown that a Pd monolayer deposited electrochemically on a Au-supported self-assembled monolayer (SAM) of 4-mercaptopyridine (Mpy) exhibits a strongly reduced Pd local density of states (LDOS) at the Fermi energy ($E_f$). Understanding the origin of this modified electronic structure is crucial for the use of the sandwich design as a platform for future nanoelectronics. Here we suggest that hydrogen adsorption might be the origin of the modified electronic properties. We performed periodic density functional theory calculation to explore the influence of hydrogen adsorption on the geometric and electronic structure of a Pd/Mpy/Au(111) complex. Dissociative adsorption of $H_2$ on a Pd monolayer on top of a Mpy SAM is a strongly exothermic process leading to atomic hydrogen atoms preferentially located at the hollow sites. Due to the formation of a strong Pd-H bond the Pd-SAM interaction realized *via* one-fold N-Pd bonds is substantially weakened. Upon hydrogen adsorption, the Pd LDOS becomes significantly modified exhibiting a drastic reduction of the density of states at $E_f$. The calculated spectra are in a good agreement with the experiment for a hydrogen coverage corresponding to two monolayers which is still thermodynamically allowed.

## I. INTRODUCTION

A new electrochemical approach [1] led recently to a successful metallization of self-assembled monolayers (SAMs) of 4-mercaptopyridine (Mpy) and 4-aminothiophenol (ATP) on Au(111) resulting in the realization of Pd/Mpy/Au [2–4], Pt/Mpy/Au [5], Rh/Mpy/Au [6], Pd/ATP/Au [7], Pt/Mpy/Pd/Mpy/Au [8] and further similar [9] sandwich systems. These can serve as prototypical units for technologies allowing communications between organic and metal components in nanoelectronics [10]. Interestingly enough, experiments based on ultraviolet photoelectron spectroscopy (UPS) revealed that the local density of states (LDOS) of the Pd layers deposited on Mpy and ATP exhibits a significant reduction near the Fermi energy ($E_f$) compared to bulk Pd, resulting in a maximum located at about -1.8 eV below $E_f$ [3, 7, 8].

To be able to design such devices in which the molecular and metal components function side by side, it is of great importance to understand the nature of the molecule-metal interface. Therefore, density functional theory (DFT) were performed [3, 8, 11–13] to elucidate the interface structure and to find the origin of the strongly modified LDOS.

Initially, a rather simple model was used to model the Pd/SAM interface [3]. The Pd-Mpy interaction was modeled by bare nitrogen atoms adsorbed on a Pd(111) monolayer with a coverage of 1/3. In such a configuration, the nitrogen atoms occupy three-fold hollow sites so that each Pd atom of the Pd layer is directly interacting with nitrogen. The strong N-Pd interaction causes a significant reduction of the Pd-LDOS at $E_f$ yielding an electronic structure in good agreement with the experiment.

Indeed, this simple model seems to be adequate to describe the essentials of the interaction of a SAM made of ATP with a hexagonal Pd monolayer according to periodic DFT calculations [11]. The amino group of ATP becomes dehydrogenated upon the ATP-Pd interaction allowing a strong bond of the nitrogen atom to the Pd monolayer in a three-fold coordination similar to bare nitrogen. As a result of this strong interaction, the Pd LDOS at the Fermi energy becomes suppressed and the maximum of the Pd density of states shifts to -1.6 eV below the Fermi energy, in good agreement with the experiment [7].

However, DFT studies revealed that the Mpy-Pd interaction in a $\sqrt{3} \times \sqrt{3}$ arrangement is much weaker than the ATP-Pd interaction. In Mpy, the nitrogen atom is located within the aromatic ring leading to a relatively weak interaction with metal layers [14]. The nitrogen atom within the pyridine ring of the Mpy molecule directly binds only to one Pd atom [8, 12, 13]. While the Pd atom directly interacting with the nitrogen atom in a one-fold coordination still exhibits a significantly modified LDOS, the electronic structure of the 2/3 of the Pd atoms of the Pd(111) monolayer not directly bound to the nitrogen atoms is hardly affected by the Pd-SAM interaction. Consequently, the calculated average density of states is at variance with the experiment.

This discrepancy between theory and experiment led finally to the concept of residual adsorbents occupying the top side of the Pd layer after processing of the junction in the electrochemical solution [11, 12]. Those molecules that are assumed to be nitrogen or sulfur-containing organic molecules primarily saturate Pd atoms not bonded to the underlying SAM resulting in a reduced DOS close to Fermi level. Indeed, introducing residual molecules into the Pd/SAM/Au model improved the agreement between theory and experiment significantly, as far as the electronic structure of the Pd layer is concerned [11].

However, such residual adsorbents have not been detected so far experimentally. Hence it is certainly fair to say that the origin of the reduced Pd density of states in Pd/Mpy/Au(111) junctions still remains unclear. Here

we suggest that hydrogen adsorption could be the cause of this reduction in the LDOS. The junctions are prepared in a aqueous environment which means that there is always a certain amount of hydrogen present. Furthermore, hydrogen interacts rather strongly with Pd [15–18]. It should also be noted that it is rather hard to detect hydrogen experimentally because hydrogen is a weak scatterer. For example, it took quite some time before the observed unsual outward relaxation of the first layer of Pd(100) [19, 20] could be related to the presence of subsurface hydrogen [21].

Hydrogen-palladium systems have been studied intensively both from an experimental [21–32] as well as from a theoretical point of view [16, 17, 33–41] as it represents a model system is surface science. At the same time, it is also relevant system for technological applications in fields such as hydrogen storage, gas sensing, or catalysis of hydrogenation reactions.

In vacuum, molecular hydrogen dissociates spontaneously on palladium surfaces occupying first the surface sites and penetrating farther into the subsurface region when coverage extends a monolayer amount [42]. Although hydrogen is a weak scatterer which makes its experimental detection not trivial, various hydrogen-induced lattice and electronic structure modifications of Pd substrates were detected [21–23, 28, 31, 32, 43, 44], e.g. adsorption induced reconstructions and anomalous multilayer relaxation effects [19–21, 30].

In the present study, we investigated the interaction of hydrogen with densely packed Pd monolayers on top of a SAM of 4-mercaptopyridine molecules formed on a Au(111) substrate. In such an arrangement, all Pd atoms are accessible to interact with hydrogen atoms. As a consequence low coordination number of the Pd atoms in the monolayer, the H-Pd$_{monolayer}$ interaction is expected to be larger than the H-Pd$_{bulk}$ interaction. Hence it is also well possible that hydrogen is present in the low pressure conditions under which the UPS measurements are performed.

This paper is structured as follows. First, the bare Pd/Mpy/Au system is discussed as the fundamental model. We elucidate the nature of the molecule-Pd bonds and its effect on the electronic structure of the Pd toplayer which consists of metallic Pd$^0$ atoms. Note that this complex is prepared in an electrochemical environment. However, since the experimental UPS experiments are carried out in ultra-high vacuum (UHV) conditions we believe that the consideration of the bare Pd/Mpy/Au system is still relevant.

In the second part, we address H/Pd/Mpy/Au(111) systems with various amount of adsorbed hydrogen. The consideration of the presence of hydrogen in the Pd/Mpy/Au system raises two fundamental questions that we are trying to answer: (i) what are the electronic and structural effects on the properties of palladium monolayer and (ii) how is the Mpy-Pd interaction affected. To elucidate these phenomena we have carried out periodic DFT calaculations for various Pd/Mpy/Au and H/Pd/Mpy/Au models. For the optimized structures the electronic structure was determined and compared to experimental UP spectra [3, 8].

## II. COMPUTATIONAL METHODS

Self-consistent periodic DFT calculations were performed employing the Vienna ab initio simulation package (VASP) [45]. To describe the exchange-correlation effects the Perdew-Burke-Ernzerhof functional[46] was used. The ionic cores were described using the projected augmented wave (PAW) method [47, 48] , and the Kohn-Sham one-electron valence states were expanded in a basis of plane waves with a cutoff energy of 400 eV. All the calculation were carried out in a spin-polarized fashion since palladium in low-dimensional structures can become magnetic [49].

The energy minimum structures of the considered Pd/Mpy/Au and H/Pd/Mpy/Au complexes were determined within a $\sqrt{3} \times \sqrt{3}$R30° surface unit cell with respect to the underlying Au(111) substrate. Thus no global lateral relaxation of the hexagonal Pd monolayer has been allowed. In this arragement, there are 4-mercaptopyridine molecule and three palladium atoms in the unit cell. The Au(111) surface was modeled by a 5-layer slab with the lower two Au layers kept frozen in their bulk position while all other atoms were allowed to relax.

To carry out the Brillouin-zone integration the method of Monkhorst and Pack [50] was employed. To sample the k-space a 11×11×1 grid was used. The structures were optimized until a convergency of $10^{-5}$ eV was reached. In order to compare the calculated local density of states (LDOS) with experimental spectra, we convoluted the LDOS with a Gaussian distribution of width 0.2 eV thus taking into account the finite energy resolution of the experimental spectra as well as the in general observed broadening of spectroscopic features due to the finite life time of the photoionized states.

## III. RESULTS AND DISCUSSIONS

### A. Bare Pd/Mpy/Au system

In this section, we address the geometric and electronic structure of a bare palladium monolayer on a Mpy-SAM deposited on Au(111). We assume a $\sqrt{3} \times \sqrt{3}$R30° arrangement with the Mpy molecules occupying the fcc near bridge sites that was previously determined as the most stable site of Mpy on Au(111) [51] as the initial structure for the deposition of the densely-packed hexagonal palladium monolayer. Such a structure corresponds to a Mpy coverage of $\frac{1}{3}$ML on Au(111), *i.e.* there is one Mpy molecule per three gold atoms in the substrate and accordingly also per three Pd atoms in the top layer.

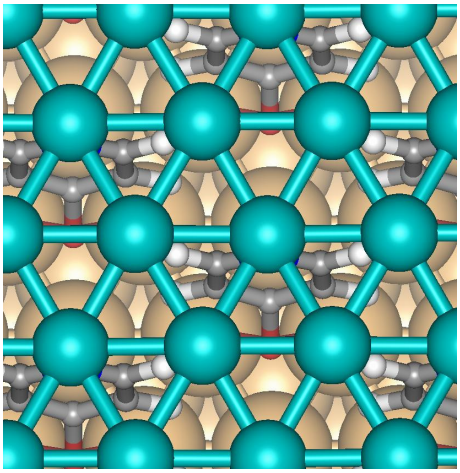

FIG. 1. Top view of the calculated optimized structure of thr palladium monolayer (light blue) deposited on top of a 4-mercaptopyridine-SAM assembled in a $\sqrt{3}\times\sqrt{3}$R30° geometry on Au(111).

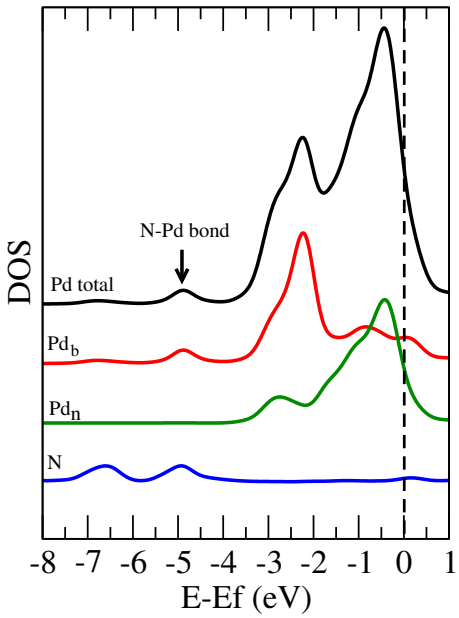


FIG. 2. Calculated local density of states (LDOS) of the Pd monolayer in the Pd/Mpy/Au model together with LDOS projected on nitrogen of Mpy molecule, palladium atom forming the N-Pd bond (Pd$_b$), and with SAM non-interacting palladium atom (Pd$_n$)

We briefly describe the nature of the Mpy-Au contact. It is realized *via* the S atom coordinated to two Au atoms in the near bridge site with a S-Au spacing of about 2.50 Å. Note that at the optimized geometry the plane of the aromatic ring of the Mpy molecule is tilted by about 34° from the surface normal. Upon the deposition of the palladium monolayer on top of the Mpy-SAM the S-Au bond is slightly prolongated by about 0.07 Å.

Although a Pd atom can form bonds to two Mpy molecules of the SAM [52], in the stable configuration of the hexagonal Pd monolayer on the SAM there is only an one-fold N-Pd bond to the Mpy-SAM on Au(111) [8]. In order to check whether the single bond is not only a consequence of the extended interatomic spacing, we also examined the N$_{molecular}$-Pd interaction within a model comprising of pyridine molecules in an up-right configuration bound to a free-standing Pd monolayer with a Pd-Pd spacing ranging from 2.6 to 2.95 Å within an 3×3 periodicity. Still, we always found the one-fold coordination to be the most preferential. Note that a similar conclusion was drawn previously for the interaction between palladim monolayer and the non-hydrogenized 4-aminothiophenol molecule [11].

The optimized structure of a palladium monolayer on top of the Mpy-SAM is illustrated in Fig. 1 where one Pd atom is directly bound to the nitrogen atom (N$_{molecular}$) of the Mpy molecule. The energy gain upon the attachment of a Pd monolayer on top of the SAM is -0.895 eV per unit cell. Note that this structure is not stable with respect to the deposition of the Pd atoms directly on the Au(111) substrate. The optimized Pd-N spacing is about 2.02 Å. As a concequence of the single Pd-Mpy bond, within the $\sqrt{3}\times\sqrt{3}$R30° unit cell there are two inequivalent types of palladium atoms: one palladium atom (Pd$_b$) is directly bound to the N$_{molecular}$ atom whereas the other two palladium atoms (Pd$_n$) are not directly interacting with the Mpy molecule. This implies that one interacting Pd$_b$ atom will be surrounded by six non-interacting Pd$_n$ atoms within the $\sqrt{3}\times\sqrt{3}$R30° arrangement as shown in Fig. 1.

In order to connect the structural motives to the electronic structure of the Pd monolayer we determined the LDOS for the optimized structures. As recently pointed out [12, 51] Jacob, the downshift of the Pd-LDOS ($\Delta$DOS$_{Pd}$) in the Pd/Mpy/Au system is rather small, $\Delta$DOS$_{Pd}$ ∼0.4 eV, which is nuch smaller than the experimentally observed value of about -1.8 eV [3]. This is demonstrated in Fig. 2 which shows that the DOS of the Pd monolayer exhibits a rather small reduction at Fermi level. There is one prominent and one minor peak within the d-band located at -0.44 and -2.2 eV, respectively, below E$_f$. Separated from the d-band, there is an additional minor peak at -4.9 eV.

The individual contributions of the two different types of Pd atoms, Pd$_b$ and Pd$_n$, to the total Pd-DOS are also included in Fig. 2. Clearly the prominent peak of the total Pd-DOS originates mainly from the Pd$_n$ atoms not directly bound to the the SAM. Furthermore, the LDOS of the Pd$_n$ atoms vanishes at about -3.5 eV with no peak visible around -4.9 eV below E$_f$. Interestingly, this LDOS qualitatively matches the theoretical LDOS spectra of a fully noninteracting free-standing palladium monolayer which has been calculated previously [3].

The LDOS spectrum projected on the Pd$_b$ atom that is directly involved in the N$_{molecular}$-Pd bond exhibits a

large reorganisation of the electronic structure compared to the noninteracting $Pd_n$ atom. The maximum of the first peak is shifted to about -3.5 eV below the Fermi energy. This feature leads to the second, smaller peak apparent in the total d-band DOS of the Pd layer. In addition, an isolated minor peak occurs at -4.9 eV below the $E_f$. A peak in the LDOS of the nitrogen atom of the Mpy molecule at the same position indicates that this feature is due to the hybridisation between states of the $Pd_b$ and $N_{molecular}$ atom leading to a covalent N-Pd bond (the corresponding state is highlighted by the arrow in Fig. 2). As illustrated in Fig. 1, the $Pd_b$ atom are located just above the nitrogen atom. This implies that the $d_{z^2}$,$d_{xz}$, and $d_{yz}$ orbitals of palladium are involved in this bond. This Pd-N interaction leads to a downshift of the $Pd_b$ d-states and consequently to a reduction of the LDOS near the Fermi energy. Still, this effect is rather local and mainly limited to the $Pd_b$ atom. The LDOS of the neighboring $Pd_n$ atoms is hardly affected by the $Pd_b$-N bond, as an inspection of the $Pd_n$ LDOS shown in Fig. 2) reveals.

In order to estimate the electron charge transfer between the individual atoms induced by the formation of the Pd-SAM-Au bonds we performed a Bader analysis [53, 54] of the electron density of the whole Pd/Mpy/Au complex. This analysis suggests that electrons from both the Au substracte and the Pd monolayer are transferred to the SAM. There is an electron surplus of about 0.230 $e$ on the Mpy molecule originated mainly from the Au→S charge transfer of about 0.167 $e$ complemented by a Pd→N charge transfer of about 0.062 $e$. Note that in the optimized Mpy/Au complex (without the Pd top layer) the Au→Mpy charge transfer is 0.195 $e$, which is slightly larger than in the Pd/Mpy/Au system suggesting that the Au-Mpy bond is slightly weakened upon the deposition of Pd monolayer on top of the SAM. This is also reflected by the slight prolongation of the Au-S bond upon the Pd deposition, as mentioned above.

Interestingly, the detailed analysis of the charges of the non-equivalent Pd atoms in the monolayer shows that there is a charge deficiency at the $Pd_b$ atom of about 0.232 $e$ whereas there is an overall charge surplus of 0.170 $e$ on the two $Pd_n$ atoms per unit cell. This shows that the Pd→Mpy charge transfer stems from the $Pd_b$ atoms with an additional $Pd_b$ →$Pd_n$ electron transfer within the palladium layer. This relatively strong inner polarization in the Pd layer will of course also affect the local chemical reactivity of the different Pd atoms.

Comparing the calculated DOS of the Pd layer with the measured UP spectrum [3] reveals large discrepancies. The experimental spectrum exhibits a reduced intensity of the DOS at the Fermi energy with the most prominent peak shifted to about -1.8 eV below $E_f$. This shows that the observed modified Pd DOS can not be explained invoking a just a bare Pd monolayer on the Mpy-SAM, as already previously realized [51, 52].

Although the one-fold N-Pd bond significantly modifies the LDOS of the $Pd_b$ atom directly bound to the SAM, the remaining two $Pd_n$ atoms per $\sqrt{3}\times\sqrt{3}$R30° unit are hardly affected by this bond. Due to the larger number of these $Pd_n$ atoms, the DOS of the Pd monolayer is dominated by the LDOS of the $Pd_n$ atoms resulting only in a small downshift of the DOS from the Fermi energy compared to bulk Pd, leading to the discrepancy with the experiment.

Because of our computational setup, in our calculations the Pd-Pd spacing is determined by the Au-Au distance of the underlying Au(111) substrate. It is not clear yet whether the Pd monolayer is really commensurate with the Au substrate. Therefore we checked the dependence of the LDOS of the Pd monolayer on the lateral Pd-Pd lattice constant [13]. We considered a free-standing Pd(111) layer with a 3×3 periodicity. Note that the optimum Pd spacing in such an isolated Pd monolayer is 2.65 Å [3]. Therefore we considered Pd-Pd distances from 2.6 to 2.95 Å with the upper value being the Au-Au bulk spacing. We calculated the Pd LDOS both for the isolated Pd layer as well as for the Pd layer covered by a $\sqrt{3}\times\sqrt{3}$ arrangement of upright standing pyridine molecules in order to mimic the influence of the N-Pd bonds [13]. Non of the calculations yielded a Pd DOS with the features found in the experiment. Hence the discrepancy between experiment and theory is not caused by a modification of the Pd-Pd lattice spacing.

### B. Hydrogen adsorption on the Pd/Mpy/Au junction

Adsorbates can rather strongly modify the electronic properties of metal surfaces and layers [51, 55, 56]. Pd is known to be easily contaminated by hydrogen [18, 21]. Furthermore, hydrogen is ubiquitous, even under very clean conditions. Hence we have studied the influence of hydrogen on the geometric and electronic structure of the Pd layer on the Mpy/Au system.

Similarly as in the case of bare Pd/Mpy/Au system we have determined the most stable configurations of the H/Pd/Mpy/Au system for various hydrogen coverages ($\Theta_H$) within a $\sqrt{3}\times\sqrt{3}$R30° periodicity. We have considered hydrogen coverages from $\Theta_H$=0.333 to 2.333 which correspond to one up to seven adsorbed hydrogen atoms per unit cell. For the optimized structures, hydrogen adsorption energies ($E_{ads}$) were evaluated with respect to the free $H_2$ molecule at various $\Theta_H$ according to

$$E_{ads} = \frac{1}{n}(E(\text{compl}+n\text{H}) - (E(\text{compl}) + \frac{n}{2}E(\text{H}_2))). \quad (1)$$

Here, $E$(compl+$n$H) is the total energy of the Pd/Mpy/Au complex with the adsorbed hydrogen and $n$ is the number of adsorbed hydrogen atoms in the unit cell.

For all considered coverages, hydrogen atoms prefer to occupy the three-fold hollow sites of the Pd(111) monolayer in order to maximize their coordination with the

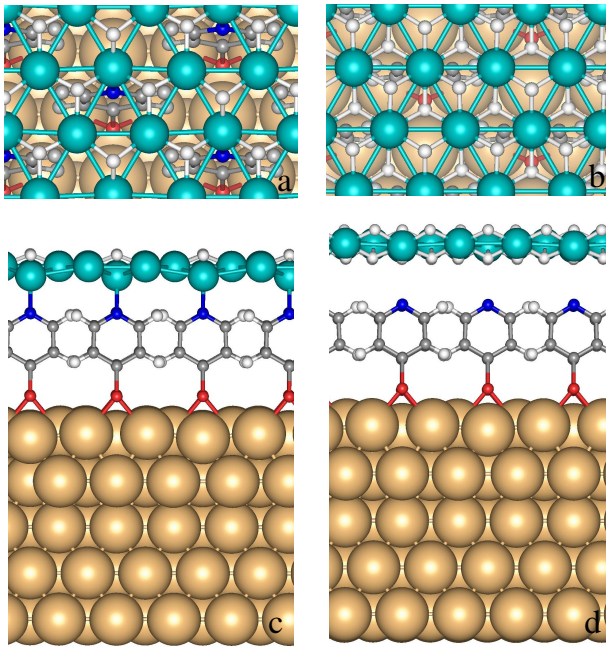


FIG. 3. Top and side view of the optimized adsorption structures of hydrogen atoms bound to the Pd monolayer of a Pd/Mpy/Au(111) junction within a $\sqrt{3} \times \sqrt{3}$R30° geometry for hydrogen coverages of $\Theta_H = 1$ (a, c) and $\Theta_H = 2$ (b, d), respectively.

Pd atoms. Note that this is similar to the Pd/Au(111) system where the both fcc and hcp hollow sites are preferentially populated [57]. At the low coverage of $\Theta_H = 1/3$, the H atoms on the surface are well separated *i.e.* the next neighbouring hollow sites around each hydrogen remain unoccupied, whereas at a hydrogen coverage of 1 monolayer (1ML, $\Theta_H = 1$) every second hollow site is occupied, as illustrated in Figs. 3a and c. If further hydrogen atoms are deposited at one of the unoccupied hollow sites, these atoms do not remain on the upper site of the layer but rather prefer to penetrate through the Pd monolayer to the lower side of the Pd layer facing the SAM. This situation is depicted for $\Theta_H$=2 in Fig. 3b and d where the hydrogen atoms form monolayers on both sides of the palladium layer. Note that in such a situation all hollow sites are occupied by H atoms.

As Fig. 3 also illustrates, the Pd-Mpy distance is substantially affected by the hydrogen adsorption on the Pd layer. This is reflected in the successive prolongation of the Pd-N bond upon increasing the hydrogen coverage (see Tab. I) starting from 2.02 Å in the bare Pd/Mpy/Au system, gradually rising to 2.21 Å at a hydrogen coverage of 1ML, followed by a jump to 3.00 Å for a coverage of 2ML. This indicates that the Pd-SAM bond becomes significantly weakened by the presence of hydrogen on the Pd layer.

This weakening is also reflected in the interaction energy ($E_{int}$) between the SAM/Au and the $n$H/Pd subsystems defined according to

$$E_{int} = E(n\text{H/Pd/Mpy/Au}) - (E(\text{Au/Mpy}) + E(\text{Pd}/n\text{H}), \quad (2)$$

where $E(n$H/Pd/Mpy/Au) is the total energy per unit cell of the H/Pd/Mpy/Au system with $n$ H atoms adsorbed on the Pd layer. $E_{int}$ drops by about 50% from -0.9 eV at $\Theta_H$=0 (no hydrogen adsorbed) to -0.42 eV at $\Theta_H$=1.0 coverage, being further reduced to -0.17 eV at a hydrogen coverage corresponding to 2ML.

This energy loss is over-compensated by the gain in hydrogen adsorption energies at different coverages listed in Tab. I. Apparently, the Pd monolayer interacts with hydrogen much stronger than the late transition metal bulk (111) substrates. In detail, at $\Theta_H$=0.333 the H atom on Pd/Mpy/Au is 1.03, 1.00, 0.44, 0.35, and 0.13 eV more strongly bound than on Au(111) [58], Ag(111) [58], Pd(111) [59], Pt(111) [58] and Pd/Au(111) [57], respectively. This is a concequence both of the extension of Pd lateral lattice constant [60, 61] and the the lower coordination of the atoms in the monolayer compared to bulk atoms [62]. As a function of coverage, the hydrogen adsorption energies decrease due to the well-known mutual repulsion between adsorbed hydrogen atoms [17]

In passing we note that the values of the interaction energy $E_{int}$ (eq. (2)) between the $n$H/Pd layer and the SAM/Au(111) system given above indicate that the deposition of Pd layer onto the SAM leads to a highly metastable system since it is energetically much more favorable to deposit the Pd atom directly on the metal substrate [63]. Still, even the hydrogen-covered Pd layers will still remain on the SAM in spite of the small adsorption energy, as long as the decomposition is kinetically hindered with sufficiently large barriers, due to the fact that a layer or larger Pd islands are in total strongly bound.

inspite of the strong reduction in the interaction energy between the Pd layer and the SAM/Au(111) system upon hydrogen adsorption, the Pd layer

So far we considered the hydrogen adsorption only with respect to the $H_2$ molecule in the gas phase. However, since experimentally the metallization of the SAM is performed in an electrochemical environment, it is of great

TABLE I. Hydrogen adsorption energy $E_{\text{ads}}$ ΔDOS, minimum Pd-N distance $d_{\text{Pd-N}}$ and position ΔDOS of the first maximum Pd LDOS below Fermi energy in the H/Pd/Mpy/Au system for various hydrogen coverages.

| $\Theta_H$ | $E_{\text{ads}}$ (eV) | $d_{\text{Pd-N}}$ (Å) | ΔDOS |
|---|---|---|---|
| 0.0 | | 2.02 | -0.44 |
| 0.333 | -0.828 | 2.09 | -0.58 |
| 0.667 | -0.792 | 2.17 | -0.63 |
| 1.0 | -0.786 | 2.21 | -0.83 |
| 1.333 | -0.678 | 2.43 | -1.13 |
| 2.0 | -0.539 | 3.01 | -2.10 |
| 2.333 | -0.362 | 3.52 | -2.52 |

importance to determine how the presence of an aqueous electrolyte and the variation of the electrode potential influence the hydrogen adsorption. Of particular interest is the equilibrium hydrogen coverage as a function of the electrode potential. Unfortunately, the realistic modeling of electrochemical electrode/electrolyte interfaces including excess charges is still computationally rather demanding [58, 59, 64–67]. Therefore we use here a procedure proposed by Nørskov *et al.* [68] in which the electrochemical conditions are taking into account within an effective thermodynamical equilibrium concept.

To be precise, here we follow the approach outlined in Ref. [64]. First, we assume that the hydrogen adsorption occurs according to the Volmer mechanism, $H^+ + e^- \rightarrow H_{ads}$. Then at equilibrium the hydrogen coverage is governed by the chemical potential of hydrogen ($\mu_H$) which can be related to the electrode potential (U) with respect to the standard hydrogen electrode (SHE) according to the relation:

$$\mu_H = -eU \tag{3}$$

Any process will proceed spontaneously if it leads to a change of the free energy $\Delta G_H < \mu_H$. Therefore we can directly relate the electrode potential with the hydrogen coverage through the differential free energy of the hydrogen adsorption [64] which can be expressed a [68]:

$$\Delta G_H = \Delta E_H + \Delta ZPE - T\Delta S. \tag{4}$$

Here, $\Delta E_H$ is the differential energy of the adsorption in the absence of any external electric field i.e., the energy gain upon the adsorption of an additional hydrogen atom. In our model, this is the energy gain upon the adsorption of the additional H atom to get from a coverage of $\Theta_H$=$n/3$ to a coverage $\Theta_H = (n+1)/3$, where $n$ is the number of H atoms in the unit cell. Note that here we assume that the adsorption energy is independent of the applied electrode potential. $\Delta$ZPE is the change of the zero-point energy upon adsorption, T is the temperature, and $\Delta$S is the change of the entropy upon adsorption. Assuming that the change of the vibrational frequencies upon adsorption depends rather weakly on the metal substrate [69] we adopted the value $\Delta$ZPE-T$\Delta$S = -0.24 eV used previously for hydrogen evolution on various metal substrate [59].

The differential free energies of hydrogen adsorption on the Pd/Mpy/Au complex as a function of the hydrogen coverage are plotted in Fig. 4. Starting at low hydrogen coverages, the curve exhibits two steps in the adsorption energy with plateaus at -0.5 eV and -0.1 eV, respectively. The first plateau corresponds to hydrogen coverages between $\Theta_H$=0.333 and $\Theta_H$=1.00. After completing 1ML of hydrogen on the Pd layer, the differential hydrogen adsorption energies exhibits a step from -0.5 to -0.1 eV. The second plateau ends at $\Theta_H$=2.0, i.e. after completion of a monolayer hydrogen coverage at the lower side of the Pd layer.

From Fig. 4, the equilibrium coverage of hydrogen as a function of the electrode potential at standard conditions can be directly read off using eq.. At $U$=0.588 V, a low hydrogen coverage of $\Theta_H$=0.333 is stable. Lowering the electrode potential to $U$=0.533 V is accompanied by an increase in the equilibrium hydrogen coverage from $\Theta_H$=0.333 to $\Theta_H$=1.0. At $U$=0.115 V, the hydrogen adsorption at the lower side of the Pd layer starts which is completed at $U$=0.053 V. For a further increase of the coverage to $\Theta_H$ >2ML, a potential drop by -0.322 V is necessary.

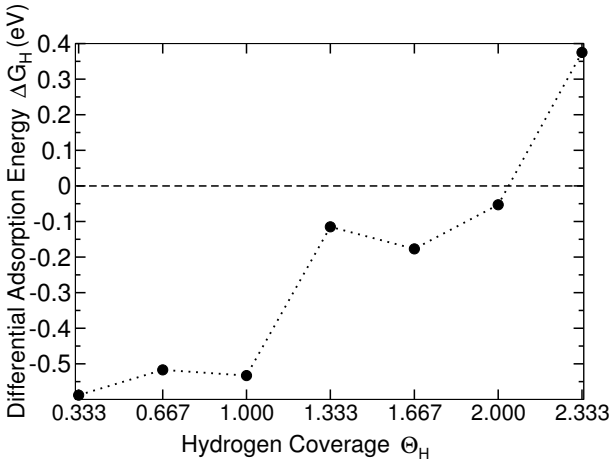


FIG. 4. Differential free energy of adsorption of hydrogen on the palladium layer of a Pd/Mpy/Au(111) complex as a function of the hydrogen coverage in a $\sqrt{3} \times \sqrt{3}$ geometry.

These number should be compared with the experimental conditions necessary for the metallization of the Mpy-SAM [1, 3, 70]. According to the plot in Fig. 4, at potentials close to $U$=0 V there will be a hydrogen coverage of 2ML present on the Pd layer. Typically, the potential scan towards the reduction of $Pd^{2+} \rightarrow Pd^0$ is started in the negative direction at +0.7 V with respect to the saturated calomel electrode (SCE), the reduction current is observed around $-0.05$ V [1]. Assuming that the SCE is shifted by +0.24 V with respect to the SHE, we find that the reduction step is occurring at a potential of $U$=+0.19 V *vs.* SHE. This is a region where the equilibrium hydrogen coverage is already above 1ML according Fig. 4 indicating that a highly covered hydrogen-palladium complex is formed immediately upon the formation of the Pd monolayer in the electrochemical solution.

We are aware that the reliability of the employed theoretical model is limited. First of all, there are no water molecules included into the model. In addition the experiment is typically carried out under the low pH conditions. Furthermore, the electrolyte also contains other anions that might interact with the palladium monolayer. However we still believe that the predicted trends in the hydrogen coverage as a function of the electrode potential are correct. For example, the adsorption energy of hydrogen is only weakly influenced by the presence of water [66].

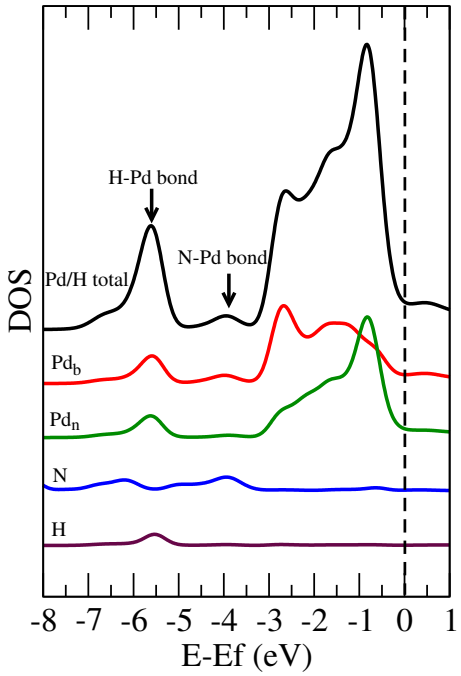


FIG. 5. Calculated LDOS of the palladium-hydrogen complex in the H/Pd/Mpy/Au system at a hydrogen coverage $\Theta_H$=1. Here, the total LDOS of the palladium-hydrogen layer (Pd/H total), the LDOS of the Pd atom bound to the nitrogen atom of the Mpy molecule ($Pd_b$), of the Pd atom not interacting with the Mpy molecules ($Pd_n$), of the nitrogen atom of Mpy (N), and of the hydrogen atom on top of the palladium layer (H) are plotted in the figure.

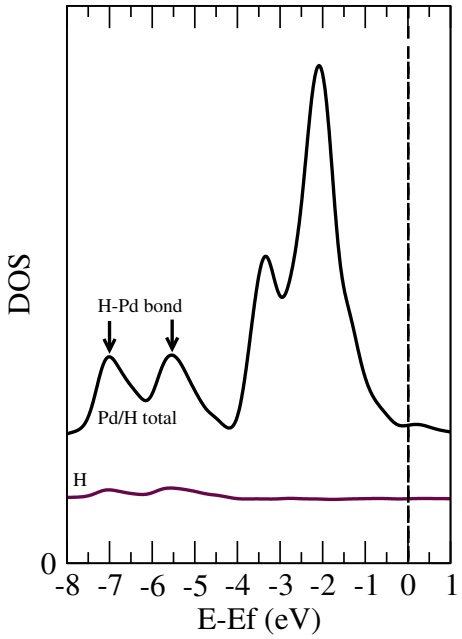


FIG. 6. Calculated LDOS of the palladium-hydrogen complex in the H/Pd/Mpy/Au system at a hydrogen coverage $\Theta_H$=2. The total DOS of the Pd layer and the LDOS of one of the hydrogen atoms are shown.

Finally, we will analyze the influence of the presence of hydrogen on the electronic structure of the palladium monolayer of the Pd/Mpy/Au junction. We have calculated the Pd-LDOS for the optimized structures of the H/Pd/Mpy/Au system for various hydrogen coverages in order to compare with the measured spectrum [3]. As just demonstrated, there is strong evidence that under the electrochemical conditions for the preparation the Pd layer is hydrogen-covered. However, the experimental spectra were obtained under UHV conditions at room temperature so that the equilibrium considerations for an electrochemical environment do not apply. Still, due to the large hydrogen adsorption energies, at least for coverages up to 1 ML (see Tab. I), hydrogen might well be present under UHV conditions. Furthermore, hydrogen is an ubiquitous contaminant, even under UHV conditions, that is in addition hard to detect. Hence we believe that our findings with respect to the influence of adsorbed hydrogen atoms are relevant for the analysis of the experimental spectra.

The calculated LDOS of the H/Pd/Mpy/Au system for hydrogen coverages of 1 ML and 2 ML are plotted in Fig. 5 and 6, respectively. At first glance it is obvious that the total DOS of the Pd layer (uppermost curves in Figs. 5 and 6) becomes substantially modified upon hydrogen adsorption. Depending on the hydrogen coverage, there is a reduction of the DOS at the Fermi energy and correspondingly a shift of the first peak to lower energies. The strong dependence of the downshift on the hydrogen coverage $\Theta_H$ is apparent from the values listed in Tab. I. In order to analyze the origin of the downshift, in Fig. 5 also the LDOS projected on the $Pd_b$, $Pd_n$, $N_{molecular}$, and a hydrogen atom of the H/Pd/Mpy/Au complex is plotted.

The H-Pd and the N-Pd interaction together lead to a splitting of the Pd d-band into three separated peaks. The peak localized at -5.6 eV is caused by the hybridization of the hydrogen s-orbital with a linear combination of the $d_{xy}$ and $d_{x^2-y^2}$ orbitals of the Pd atoms The peak related to the Pd-N bond is located at -3.9 eV below $E_f$ which is about 1 eV higher in energy compared to the uncovered palladium layer on top of the SAM. The electronic structure of the $Pd_n$ atoms is not affected by the $Pd_b$-N interaction, as already found for the bare Pd layer.

Upon the adsorption of additional hydrogen beyond 1ML coverage at the lower side of the Pd layer, the Pd–H related features in the LDOS are split into two peaks. For a hydrogen coverage of 2ML the peak positions are -5.6 and -7.03 eV below the Fermi energy, as Fig. 6 shows. Interestingly enough, the features related to the Pd-N interaction vanish which makes sense regarding the enlarge Pd-N distance of 3 Å at $\Theta_H = 2.0$.

In order to monitor the charge transfer within the H/Pd/Mpy/Au complex, we have also carried out a Bader analysis [53, 54] for hydrogen coverages $\Theta_H = 1.0$

and $\Theta_H$ = 2.0. There is a electron deficiency of 0.180 and 0.187 $e$ at the Au atoms at 1ML and 2ML coverages, respectively, which is slightly larger than for the uncovered Pd layer. This indicates that the Au-Mpy bond is becoming stronger upon the hydrogen-induced weakening of the Pd-Mpy interaction. Correspondingly, the Au-S bond length is slightly shortened from 2.57 to 2.56 and 2.53 Å at hydrogen coverages of $\Theta_H$=0, 1, and 2, respectively. There is a charge accumulation at the Mpy molecule of 0.267 and 0.250 $e$ at $\Theta_H$=1 and $\Theta_H$=2, respectively, and a corresponding charge depletion of 0.087 and 0.063 $e$ in the Pd/H subsystem.

So far we have again assumed that the Pd layer is pseudomorphic with respect to the underlying Au(111) substrate. In order to check the influence of the lateral spacing on the properties of the hydrogen-covered Pd layer, we used a free-standing Pd monolayer within a 3×3 periodicity. For various hydrogen coverages we determined the optimum Pd-Pd distance and the corresponding electronic structure. The results are summarized in Tab. II. Interestingly enough, the optimized Pd-Pd distance for $\Theta_H$=2.0 is rather close to the nearest-neighbor distance in bulk Au. Also the position $\Delta DOS$ of the first peak in the Pd LDOS calculated for the full H/Pd/Mpy/Au(111) complex (Tab. I) and the H/Pd$_{ML}$ (Tab. II) as a function of the hydrogen coverage are pretty close. This gives confidence that the assignment of the peak position as a function of the hydrogen coverage is semi-quantitatively correct, independent of the particular model used.

Finally we compare the calculated total LDOS of the palladium monolayer with the corresponding measured palladium UPS spectra [3]. Upon the consideration of the adsorbed hydrogen atom the theoretical spectra exhibit a reduced DOS at the Fermi level in agreement with the experiment. Interestingly enough, for a hydrogen coverage of 2ML the calculated downshift of the prominent peak is about -2.10 eV which agrees well with the experimental value of -1.8 eV. Since the dissociative adsorption of $H_2$ molecules on the Pd/Mpy/Au junction is strongly exothermic, we think that it is very likely that the hydrogen coverage on the Pd layer persists even under the UHV conditions of the UPS measurements, as already mentioned in the beginning of section III B and thus is the cause for the experimentally observed downshift of the Pd LDOS [3]. Another consequence of the formation of the hydrogen adlayer on the Pd is the weakened interaction between the SAM and the Pd layer. This means that the electronic properties of the deposited Pd layer are rather independent of the particular molecules the SAM is made of. Thus the electronic structure of Pd layers on top of different SAMs should be similar. We believe that this provides an explanation for the experimental observation that the UPS spectra of the Pd monolayers of Pd/4-mercaptopyridine/Au(111) [3] and Pd/4-aminothiophenol/Au [7] junctions hardly differ since the electronic structure is not dominated by the Pd-SAM interaction but rather by the H-Pd interaction.

Unfortunately, any direct experimental evidence of hydrogen on the Pd/Mpy/Au(111) system is still missing. Still, there is both experimental [22, 23] and theoretical [71] information available about the influence of a hydrogen adlayer on bulk Pd(111). Interestingly enough, these studies show a drastic reduction of the LDOS of the first Pd layer at the Fermi energy which is similar to the one observed for the Pd/SAM/Au junctions. This might be another indirect argument supporting the proposal that hydrogen adsorption is the main reason for such large downshift of the palladium DOS in Pd/SAM/Au junctions.

TABLE II. Optimized Pd-Pd distances and the position of the maximum of the first band of calculated Pd LDOS relative to Fermi energy as a function of the hydrogen coverage for a free-standing palladium monolayer within a 3×3 periodicity.

| $\Theta_H$ | $d_{Pd-Pd}$ (Å) | $\Delta DOS$ (eV) |
|---|---|---|
| 0 | 2.63 | -0.38 |
| 0.111 | 2.65 | -0.43 |
| 0.333 | 2.67 | -0.44 |
| 0.667 | 2.71 | -0.73 |
| 1.000 | 2.75 | -1.16 |
| 2.000 | 2.90 | -2.14 |

## IV. CONCLUSIONS

We have used periodic density functional theory to study the influence of hydrogen adsorption on the electronic and geometric structure of Pd/Mpy/Au junctions. Adsorbed hydrogen atoms preferentially occupying the three-fold hollow sites interact strongly with the densely packed palladium monolayer bound to the $\sqrt{3} \times \sqrt{3}$R30° 4-mercaptopyridine-SAM adsorbed on Au(111). Under electrochemical conditions, the Pd layer on top of the SAM is covered on both sides by hydrogen corresponding to a nominal hydrogen coverage of 2ML. The adsorption of hydrogen leads to a substantial weakening of the Pd-SAM bond. The high hydrogen adsorption energy also makes it very likely that hydrogen atoms remain on the Pd layer even under ultra-high vacuum conditions.

The presence of hydrogen on the Pd layer leads to a substantial reduction of the Pd local density of states and a downshift of the first peak in the LDOS that depends on the hydrogen coverage. At a coverage corresponding to two monolayers of hydrogen the first peak in the Pd density of states appears at -2.1 eV below the Fermi energy in a good agreement with the experimentally observed value of -1.8 eV. These findings suggest that it might well possible that the observed downshift of the density of states of Pd layers deposited electrochemically on self-assembled monolayers are caused by the presence of hydrogen attached to the Pd layer.

**ACKNOWLEDGEMENT**

Financial support by the Deutsche Forschungsgemeinschaft (DFG) within SFB 569 is gratefully acknowledged. Computational resources have been provided by the bwGRiD project of the Federal State of Baden-Württemberg/ Germany. Fruitful discussions with Hans-Gerd Boyen and Dieter Kolb are gratefully acknowledged.

[1] Ivanova, V.; Baunach, T.; Kolb, D. M. *Electrochim. Acta* **2005,** *50,* 4283.
[2] Baunach, T.; Ivanova, V.; Kolb, D. M.; Boyen, H.-G.; Ziemann, P.; Büttner, M.; Oelhafen, P. *Adv. Mater.* **2004,** *16,* 2024.
[3] Boyen, H.-G.; Ziemann, P.; Wiedwald, U.; Ivanova, V.; Kolb, D. M.; Sakong, S.; Groß, A.; Romanyuk, A.; Büttner, M.; Oelhafen, P. *Nature Mater.* **2006,** *5,* 394.
[4] Shekhah, O.; Busse, C.; Bashir, A.; Turcu, F.; Yin, X.; Cyganik, P.; Birkner, A.; Schuhmann, W.; Wöll, C. *Phys. Chem. Chem. Phys.* **2006,** *8,* 3375-3378.
[5] Manolova, M.; Ivanova, V.; Kolb, D. M.; Boyen, H.-G.; Ziemann, P.; Büttner, M.; Romanyuk, A.; Oelhafen, P. *Surf. Sci.* **2005,** *590,* 146.
[6] Manolova, M.; Kayser, M.; Kolb, D. M.; Boyen, H.-G.; Ziemann, P.; Mayer, D.; Wirth, A. *Electrochim. Acta* **2007,** *52,* 2740-2745.
[7] Manolova, M.; Boyen, H.-G.; Kučera, J.; Groß, A.; Romanyuk, A.; Oelhafen, P.; Ivanova, V.; Kolb, D. M. *Adv. Mater.* **2009,** *21,* 320.
[8] Eberle, F.; Saitner, M.; Boyen, H.-G.; Kučera, J.; Groß, A.; Romanyuk, A.; Oelhafen, P.; D'Olieslaeger, M.; Manolova, M.; Kolb, D. M. *Angew. Chem. Int. Ed.* **2010,** *49,* 341-345.
[9] Silien, C.; Lahaye, D.; Caffio, M.; Schaub, R.; Champness, N. R.; Buck, M. *Langmuir* **2011,** *27,* 2567-2574.
[10] McCreery, R. L.; Bergren, A. J. *Adv. Mater.* **2009,** *21,* 4303.
[11] Kučera, J.; Groß, A. *Phys. Chem. Chem. Phys.* **2010,** *12,* 4423.
[12] Keith, J. A.; Jacob, T. *Electrochimica Acta* **2010,** *55,* 8258 - 8262.
[13] Kučera, J.; Groß, A. *Beilstein J. Nanotech.* **2011,** *2,* 384-393.
[14] Tonigold, K.; Groß, A. *J. Chem. Phys.* **2010,** *132,* 224701.
[15] Christmann, K. *Surf. Sci. Rep.* **1988,** *9,* 1.
[16] Dong, W.; Ledentu, V.; Sautet, P.; Eichler, A.; Hafner, J. *Surf. Sci.* **1998,** *411,* 123.
[17] Lischka, M.; Groß, A. *Phys. Rev. B* **2002,** *65,* 075420.
[18] Pundt, A.; Kirchheim, R. *Annu. Rev. Mater. Res.* **2006,** *36,* 555-608.
[19] Behm, R.; Christmann, K.; Ertl, G.; Hove, M. V.; Thiel, P.; Weinberg, W. *Surf. Sci.* **1979,** *88,* L59.
[20] Quinn, J.; Li, Y. S.; Tian, D.; Li, H.; Jona, F.; Marcus, P. M. *Phys. Rev. B* **1990,** *42,* 11348.
[21] Kim, S. H.; Meyerheim, H. L.; Barthel, J.; Kirschner, J.; Seo, J.; Kim, J.-S. *Phys. Rev. B* **2005,** *71,* 205418.
[22] Conrad, H.; Ertl, G.; Küppers, J.; Latta, E. *Surf. Sci.* **1976,** *58,* 578.
[23] Demuth, J. *Surf. Sci.* **1977,** *65,* 369.
[24] Behm, R. J.; Christmann, K.; Ertl, G. *Surf. Sci.* **1980,** *99,* 320.
[25] Eberhardt, W.; Greuter, F.; Plummer, E. W. *Phys. Rev. Lett.* **1981,** *46,* 1085.
[26] Eberhardt, W.; Louie, S. G.; Plummer, E. W. *Phys. Rev. B* **1983,** *28,* 465.
[27] Behm, R. J.; Penka, V.; Cattania, M.-G.; Christmann, K.; Ertl, G. *J. Chem. Phys.* **1983,** *78,* 7486.
[28] Kampshoff, E.; Waelchli, N.; Menck, A.; Kern, K. *Surf. Sci.* **1996,** *360,* 55.
[29] Wetzig, D.; Rutkowski, M.; Zacharias, H.; Groß, A. *Phys. Rev. B* **2001,** *63,* 205412.
[30] Di Vece, M.; Grandjean, D.; Van Bael, M. J.; Romero, C. P.; Wang, X.; Decoster, S.; Vantomme, A.; Lievens, P. *Phys. Rev. Lett.* **2008,** *100,* 236105.
[31] Tew, M. W.; Miller, J. T.; van Bokhoven, J. A. *J. Phys. Chem. C* **2009,** *113,* 15140.
[32] Yoshinobu, J.; Tanaka, H.; Kawai, M. *Phys. Rev. B* **1995,** *51,* 4529.
[33] Ozawa, N.; Roman, T. A.; Nakanishi, H.; Kasai, H. *J. Appl. Phys.* **2007,** *101,* 123530.
[34] Tománek, D.; Wilke, S.; Scheffler, M. *Phys. Rev. Lett.* **1997,** *79,* 1329.
[35] Dong, W.; Kresse, G.; Furthmüller, J.; Hafner, J. *Phys. Rev. B* **1996,** *54,* 2157.
[36] Groß, A. *ChemPhysChem* **2010,** *11,* 1374.
[37] Groß, A. *Surf. Sci.* **1996,** *363,* 1.
[38] Groß, A.; Scheffler, M. *Phys. Rev. B* **1998,** *57,* 2493.
[39] Busnengo, H. F.; Dong, W.; Salin, A. *Chem. Phys. Lett.* **2000,** *320,* 328.
[40] Busnengo, H. F.; Dong, W.; Sautet, P.; Salin, A. *Phys. Rev. Lett.* **2001,** *87,* 127601.
[41] Olsen, R. A.; Philipsen, P. H. T.; Baerends, E. J.; Kroes, G. J.; Løvvik, O. M. *J. Chem. Phys.* **1997,** *106,* 9286.
[42] Muschiol, U.; Schmidt, P. K.; Christmann, K. *Surf. Sci.* **1998,** *395,* 182.
[43] Ingham, B.; Toney, M. F.; Hendy, S. C.; Cox, T.; Fong, D. D.; Eastman, J. A.; Fuoss, P. H.; Stevens, K. J.; Lassesson, A.; Brown, S. A.; Ryan, M. P. *Phys. Rev. B* **2008,** *78,* 245408.
[44] Davis, R. J.; Landry, S. M.; Horsley, J. A.; Boudart, M. *Phys. Rev. B* **1989,** *39,* 10580.
[45] Kresse, G.; Furthmüller, J. *Phys. Rev. B* **1996,** *54,* 11169.
[46] Perdew, J. P.; Burke, K.; Ernzerhof, M. *Phys. Rev. Lett.* **1996,** *77,* 3865.
[47] Blöchl, P. E. *Phys. Rev. B* **1994,** *50,* 17953.
[48] Kresse, G.; Joubert, D. *Phys. Rev. B* **1999,** *59,* 1758.
[49] Groß, A. *Theoretical surface science – A microscopic perspective;* Springer: Berlin, 2nd ed.; 2009.
[50] Monkhorst, H. J.; Pack, J. D. *Phys. Rev. B* **1976,** *13,* 5188.
[51] Kučera, J.; Groß, A. *Langmuir* **2008,** *24,* 13985.
[52] Keith, A. B.; Jacob, T. *Chemistry - A European Journal* **2010,** *16,* 12381.

[53] Bader, R. F. W. *Atoms in Molecules - A Quantum Theory;* Oxford University Press: Oxford, 1990.

[54] Henkelman, G.; Arnaldsson, A.; Jónsson, H. *Comput. Mater. Sci.* **2006,** *36,* 254.

[55] Hammer, B. *Phys. Rev. B* **2001,** *63,* 205423.

[56] Wei, C. M.; Groß, A.; Scheffler, M. *Phys. Rev. B* **1998,** *57,* 15572.

[57] Roudgar, A.; Groß, A. *J. Electroanal. Chem.* **2003,** *548,* 121.

[58] Schnur, S.; Groß, A. *Catal. Today* **2011,** *165,* 129-137.

[59] Nørskov, J. K.; Bligaard, T.; Logadottir, A.; Kitchin, J. R.; Chen, J. G.; Pandelov, S.; Stimming, U. *J. Electrochem. Soc.* **2005,** *152,* J23.

[60] Mavrikakis, M.; Hammer, B.; Nørskov, J. K. *Phys. Rev. Lett.* **1998,** *81,* 2819.

[61] Groß, A. *J. Phys.: Condens. Matter* **2009,** *21,* 084205.

[62] Groß, A. *J. Comput. Theor. Nanosci.* **2008,** *5,* 894.

[63] Roudgar, A.; Groß, A. *Surf. Sci.* **2005,** *597,* 42.

[64] Skúlason, E.; Karlberg, G. S.; Rossmeisl, J.; Bligaard, T.; Greeley, J.; Jónsson, H.; Nørskov, J. K. *Phys. Chem. Chem. Phys.* **2007,** *9,* 3241.

[65] Taylor, C. D.; Wasileski, S. A.; Filhol, J.-S.; Neurock, M. *Phys. Rev. B* **2006,** *73,* 165402.

[66] Roudgar, A.; Groß, A. *Chem. Phys. Lett.* **2005,** *409,* 157.

[67] Schnur, S.; Groß, A. *New J. Phys.* **2009,** *11,* 125003.

[68] Nørskov, J. K.; Rossmeisl, J.; Logadottir, A.; Lindqvist, L.; Kitchin, J. R.; Bligaard, T.; Jónsson, H. *J. Phys. Chem. B* **2004,** *108,* 17886-17892.

[69] Bligaard, T.; Honkala, K.; Logadottir, A.; Nørskov, J. K.; Dahl, S.; Jacobsen, C. J. H. *J. Phys. Chem. B* **2003,** *107,* 9325-9331.

[70] Baunach, T.; Ivanova, V.; Scherson, D. A.; Kolb, D. M. *Langmuir* **2004,** *20,* 2797.

[71] Dong, W.; Hafner, J. *Phys. Rev. B* **1997,** *56,* 15396.